

# An Integrated Sensitivity Analysis for the Basalt Specific Multicomponent Geothermometer for High Temperature Settings

Lars H. Ystroem, Fabian Nitschke, Sebastian Held, Thomas Kohl

Karlsruhe Institute of Technology (KIT), Institute of Applied Geosciences, Division of Geothermic, Adenauerring 20b, 76131  
Karlsruhe, Germany

lars.ystroem@kit.edu, fabian.nitschke@kit.edu, sebastian.held@kit.edu, thomas.kohl@kit.edu

**Keywords:** sensitivity analysis, multicomponent geothermometry, reservoir temperature estimation, Krafla geothermal system, Mult\_predict

## ABSTRACT

For a successful geothermal reservoir exploration, an *in-situ* temperature estimation is essential. Since geothermometric reservoir temperature estimations often entail high uncertainties, statistical approaches are used. The focus is on the application of sensitive analyses on a basalt specific mineral set as multicomponent geothermometer to estimate the reservoir temperatures in Krafla, high-temperature geothermal field, Iceland.

In quantitative geothermometry, the element ratios and mineral saturation of the geothermal fluid serve as single geothermometers. The geochemical equilibrium between mineral phases and the reservoir rock are used to obtain the reservoir temperature. The coupling of several minerals serving as a multicomponent geothermometer allows for statistically robust temperature estimations. Herein, we set up a specific mineral set for basaltic reservoir rocks, which are calibrated by *in-situ* measurements of the reservoir temperature in Krafla. The developed method uses IPHREEQC to determine the geochemical equilibrium conditions, followed by the statistical evaluation conducted with a Matlab-based in-house tool called Mult\_predict. The results are presented via box plots. The evaluation of the dataset from Krafla allows the calibration of a basalt specific mineral set for the most accurate reservoir temperature estimation. As surface measurements of pH, aluminum concentration and steam loss do not reflect reservoir conditions, further sensitivity analyses are combined to back-calculate these parameters in order to improve the temperature estimation. This statistical evaluation reflects the most plausible reservoir conditions. It is shown that, the variation of the redox potential, iron and magnesium concentration have only negligible effects and thus can be discarded, the correct determination of the *in-situ* pH, aluminum concentration and steam loss are essential for a robust temperature estimation. The calculated reservoir temperature matches the measured *in-situ* reservoir temperature with an overall spread of 1.7% of the total measured median temperature. In conclusion, the developed method is a promising tool for the estimation of reservoir temperatures. In addition, it is an economical exploration tool that allows a high precision temperature estimation. Since the developed basalt specific multicomponent geothermometer also uses secondary mineralization it could be adapted to different geothermal settings, although requiring further calibration and validation.

## 1. INTRODUCTION

Reservoir temperature estimation is a key technique in successful geothermal reservoir exploration. Quantitative solute geothermometry provides such temperature estimations. The coupling of multiple mineral phases as a multicomponent geothermometer was introduced by Reed and Spycher (1984). They plotted the saturation curves of multiple minerals against temperature. For this purpose, the saturation indices of multiple mineral phases have to be calculated over a certain temperature range (Equation 1).

$$SI(T) = \log \left( \frac{IAP}{K(T)} \right) \quad (1)$$

$SI$  is the temperature-dependent saturation index of a mineral phase,  $IAP$  is the ion activity product and  $K$  the temperature-dependent thermodynamic equilibrium constant of one mineral phase. Only in the case  $SI$  equals zero, the equilibrium state between the reservoir fluid and the mineral phase is reached and can be evaluated. Thus, temperatures at which mineral phases reach equilibrium can be used for reservoir temperature estimation. Nevertheless, this result is prone to uncertainties. Changes in the chemistry of the fluid can lead to divergences of the initial equilibrium conditions in the reservoir. While the fluid ascends to the earth surface, it is vulnerable to secondary processes such as boiling, phase segregation, mixing or dilution and precipitation (Arnórsson et al. 1990; Cooper et al. 2013; Peiffer et al. 2014; Spycher et al. 2014). Therefore, additional sensitivity analyses can be performed to reconstruct reservoir conditions. The aim is to vary multiple sensitive parameters around their initial value to find a minimum in the calculated temperature estimation spread. At this point, the equilibrium state ( $SI = 0$ ) of the mineral phases have the smallest distances between each other and thus, the minimum in the sensitivity field is reached. Phases, which do not reach the equilibrium are excluded from the calculations.

## 2. METHOD AND RESULTS

With the help of the developed basalt specific mineral set, it is possible to calculate robust temperature estimations. The set contains mineral phases found in the basaltic geology of Krafla, which is described by Arnórsson et al. (1983). These mineral phases are extended by secondary minerals, which generally occur in geothermal systems (Giggenbach 1981). The developed basalt specific mineral set is listed in Appendix 1. For the sensitivity analyses, the used mineral phases have to be stable throughout the variation. Hence, the saturations indices of a mineral phase have to be calculated throughout a temperature range of 20°C to 300°C while each sensitive parameter is varied around its initial value. Static boundary conditions like the consistency of mineral phases are essential

for the latter statistical evaluation. In the sensitivity analyses, the minimum in the temperature distribution of each parameter is determined. The variation of the sensitive parameter has to be chosen large enough to not only find a local minimum, but instead to find the global minimum. The integration of the sensitivity analyses considers the geochemical dependence of these sensitive parameters. Giggenbach (1981, 1988) proposed that changes in the partial pressure of  $\text{CO}_2$  and  $\text{H}_2\text{S}$  results in pH changes and buffer reactions in the fluid. This degassing effect occurs due to temperature and pressure changes while ascent of the fluid and the sampling process. In addition, the pH value is temperature-dependent which also shifts the value before analysing in the laboratory. Furthermore, steam loss controls the pH value. This is taken into account by performing a sensitivity analysis for steam loss as well as pressure relief causes boiling. Furthermore, the pH value is vulnerable to measuring errors. Nitschke et al. (2017) and Reed and Spycher (1984) are aware of these problems and suggest to measure the pH value directly in the field and later on in the laboratory to reconstruct the pH value at reservoir conditions. Likewise, Giggenbach (1981) used the thermodynamic stability of aluminosilicates for reservoir temperature estimation. In conclusion, pH shifts can lead to changes in the aluminum concentration. Aluminosilicates have a strong tendency to precipitate in several phases. These buffer reactions in the fluid can form aluminum complexes, which are likely to precipitate. Therefore, complexes get lost with the ascent of the fluid. Also, the aluminum concentration is vulnerable to fluid sampling. While sampling, these complexes are filtered because their size exceeds the usually used  $0.2 \mu\text{m}$  filter membrane. Likewise, the measured aluminum concentrations in the fluid are close to the detection limit, which leads to additional uncertainties. Hence, minimal changes in the concentration cause large effects of increasing or decreasing the solubility product and thus, to huge uncertainties in temperature estimations. Furthermore, the redox potential is coupled to the pH value. The lower boundary of the redox potential in geothermal fluids is defined by the standard potential of hydrogen, consequently the pH value. The upper limit is given by the strongest naturally occurring oxidant which is oxygen. The iron-bearing minerals of the basalt specific mineral set (e.g. hematite, goethite, pyrite) are redox state-dependent. Also, the measured iron and magnesium concentrations are close to the detection limit. The variations of these sensitive parameters is visualised in Figure 1. The figure comprises the pH value, aluminum concentration, steam loss, redox potential as well as iron and magnesium concentration. Especially the pH value, the aluminum concentration and the steam loss are vulnerable to changes. Whereas variations of the redox potential, the iron and magnesium concentration have negligible sensitivity on the equilibrium temperature distribution of the mineral set. Due to the marginal effects, the sensitivity analysis of the redox potential, as well as for the iron and magnesium concentration can be omitted for future temperature estimation.

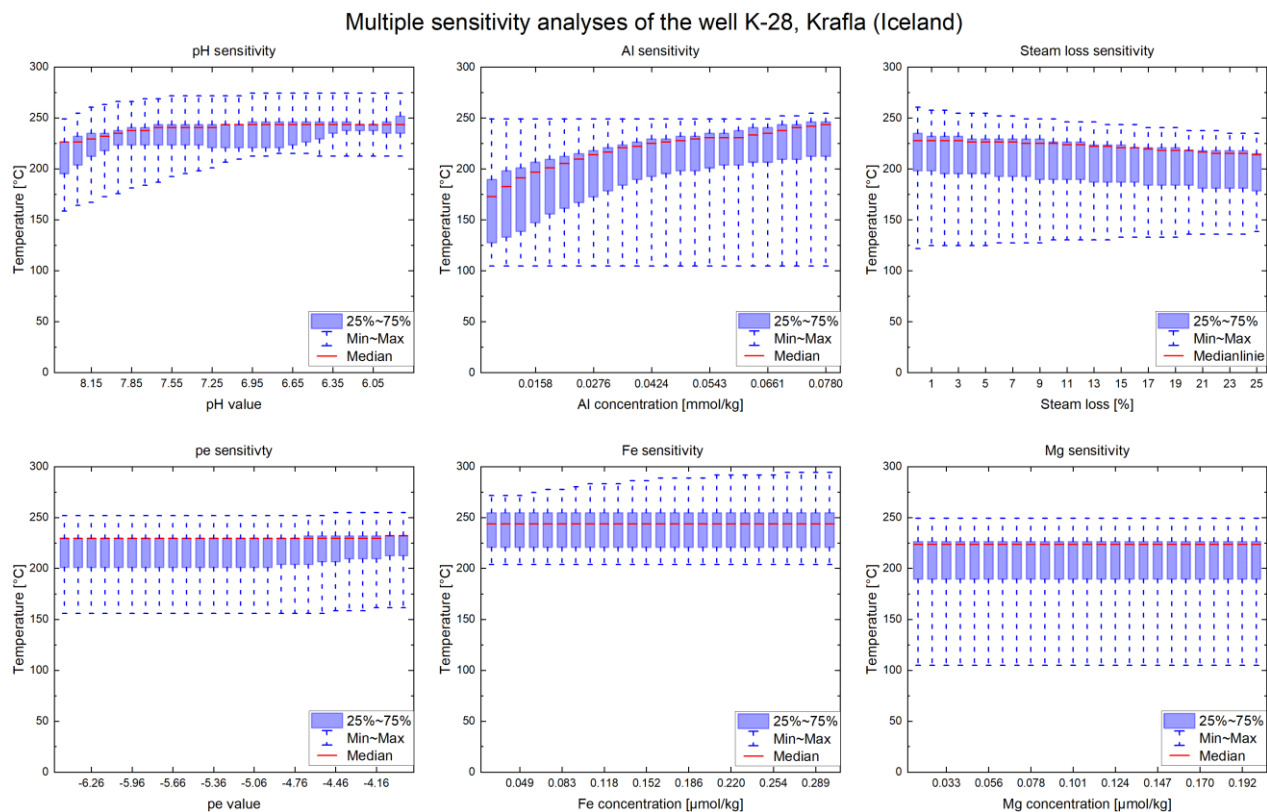


**Figure 1: Visualisation of multiple sensitivity analyses for different sensitive parameters (pH, aluminum concentration, steam loss, redox potential, iron and magnesia concentration).**

Therefore, pH, aluminum concentration and steam loss are the most sensitive parameters, which should be analysed to obtain the most realistic reservoir conditions. Due to the major amount of aluminosilicates as multicomponent geothermometer in the basalt specific mineral set (Appendix 1), these three sensitivity analyses have to be combined and varied interdependently. The integrated sensitivity analysis of pH, aluminum concentration and steam loss is implemented in an in-house tool called `MuT_predict`. The Matlab-based software uses `IPhreeqc` (Parkhurst and Appelo 2013) to calculate the saturation indices of the mineral phases of the basalt specific mineral set (Appendix 1). Each sensitive parameter is varied over all variation steps of the other parameters. Hence, a three-dimensional cell-array is calculated. An entry of the array contains the equilibrium temperatures of all consistent mineral phases. These temperature estimations were statistically evaluated to find the minimal distance within the temperature spread. Figure 2 shows the differences of this temperature spread for a static steam loss amount over the variation of aluminum concentration and pH. The morphology of the temperature distribution reflects one layer of the three-dimensional cell-array. At the global minimum the

temperature spread of the mineral phases is the smallest. This point resembles the reservoir conditions for all sensitive parameters. Exemplarily, for the well K-28 (data by Guðmundsson and Arnórsson (2002)), the minimum is reached at an aluminum concentration of 0,79 mmol/kg and a pH value of 7.95. The selected layer was calculated for a steam loss of 14%. Compared to the initial values of the geochemical analysis (Al concentration: 0.033 mmol/kg, pH: 9.55) the parameters markedly shifted.

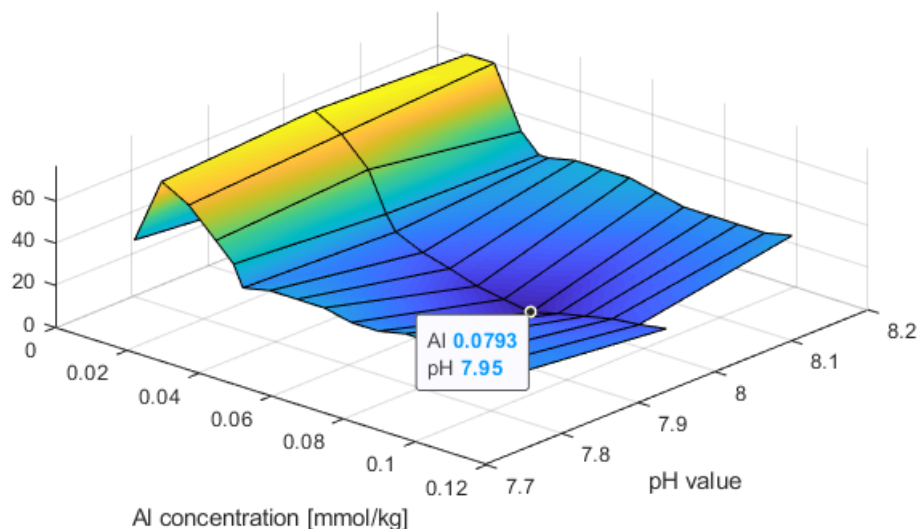


**Figure 2: Sensitivity field for the well K-28, Krafla (Iceland). The field is spanned between the aluminum concentration and the pH value. The layer was calculated for a steam loss of 14%. The minimum resembles the reservoir conditions at pH 7.95 and an aluminum concentration of 0.079 mmol/kg.**

#### 4. DISCUSSION

Consequently, the calculated temperature estimation can be compared to the measured *in-situ* temperatures, exemplarily of the well K-28 in Krafla. Guðmundsson and Arnórsson (2002) identified two permeable horizons, which feed the borehole. These aquifers are located at a depth of 500 m and 800 m beneath ground level. Their measured inflow temperature is 230°C respectively 240°C. Figure 3 visualises the improvement of the reservoir temperature estimations by performing the integrated sensitivity analysis. The first box plot shows the temperature estimation by only using the basalt specific mineral set (Appendix 1). After the application of the integrated sensitivity analysis the temperature estimations box plot gains a tremendous amount of precision. The overall spread of the box plot minimizes to 1.7% of the absolute median temperature estimation. The orange bar corresponds the measured *in-situ* temperature range. The optimized temperature estimation fits this range precisely.

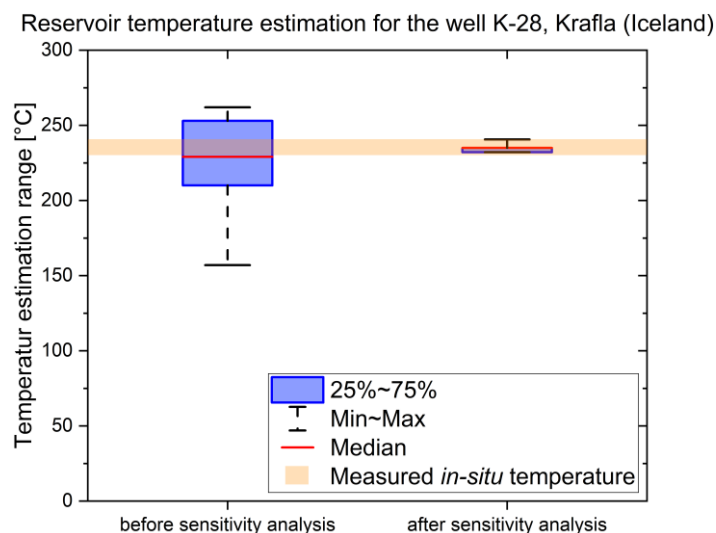


**Figure 3: Reservoir temperature estimations for the well K-28 using the basalt specific mineral set (Appendix 1). The first column shows the temperature estimation before applying the integrated sensitivity analysis (pH, aluminum concentration and steam loss). The second column visualises the temperature estimation after performing the integrated sensitivity analysis. The orange bar indicates the measured *in-situ* temperatures given by Guðmundsson and Arnórsson (2002).**

In conclusion, the combination of multiple sensitivity analyses (pH, aluminum concentration and steam loss) results in a precise and robust application. By varying sensitive parameters around their initial value, reservoir conditions can be reconstructed. For this purpose, the in-house tool Mult\_predict statistically evaluates the calculated temperature estimations and finds the global minimum

in temperature spread. Thus, the integrated sensitivity analysis markedly improves the temperature estimations of the basalt specific mineral set.

## REFERENCES

- Arnórsson S, Gunnlaugsson E, Svavarsson H (1983) The chemistry of geothermal waters in Iceland. II. Mineral equilibria and independent variables controlling water compositions. *Geochimica et Cosmochimica Acta* 47:547–566. doi: 10.1016/0016-7037(83)90277-6
- Arnórsson S, Björnsson S, Muna ZW, Bwire-Ojiambo S (1990) The use of gas chemistry to evaluate boiling processes and initial steam fractions in geothermal reservoirs with an example from the olkaria field, Kenya. *Geothermics* 19:497–514. doi: 10.1016/0375-6505(90)90002-S
- Cooper DC, Palmer CD, Smith RW, McLing TL (2013) Multicomponent Equilibrium Models for Testing Geothermometry Approaches. 38th Workshop on Geothermal Reservoir Engineering
- Giggenbach WF (1981) Geothermal mineral equilibria. *Geochimica et Cosmochimica Acta* 45:393–410. doi: 10.1016/0016-7037(81)90248-9
- Giggenbach WF (1988) Geothermal solute equilibria. Derivation of Na-K-Mg-Ca ge indicators. *Geochimica et Cosmochimica Acta* 52:2749–2765. doi: 10.1016/0016-7037(88)90143-3
- Guðmundsson BT, Arnórsson S (2002) Geochemical monitoring of the Krafla and Námafjall geothermal areas, N-Iceland. *Geothermics* 31:195–243. doi: 10.1016/S0375-6505(01)00022-0
- Nitschke F, Held S, Villalon I, Neumann T, Kohl T (2017) Assessment of performance and parameter sensitivity of multicomponent geothermometry applied to a medium enthalpy geothermal system. *Geotherm Energy* 5:1. doi: 10.1186/s40517-017-0070-3
- Parkhurst DL, Appelo CAJ (2013) Description of Input and Examples for PHREEQC Version 3—A Computer Program for Speciation, Batch-Reaction, One-Dimensional Transport, and Inverse Geochemical Calculations. U.S. Geological Survey Techniques and Methods:497 p.
- Peiffer L, Wanner C, Spycher N, Sonnenthal EL, Kennedy BM, Iovenitti J (2014) Optimized multicomponent vs. classical geothermometry: Insights from modeling studies at the Dixie Valley geothermal area. *Geothermics* 51:154–169. doi: 10.1016/j.geothermics.2013.12.002
- Reed MH, Spycher N (1984) Calculation of pH and mineral equilibria in hydrothermal waters with application to geothermometry and studies of boiling and dilution. *Geochimica et Cosmochimica Acta* 48:1479–1492. doi: 10.1016/0016-7037(84)90404-6
- Spycher N, Peiffer L, Sonnenthal EL, Saldi G, Reed MH, Kennedy BM (2014) Integrated multicomponent solute geothermometry. *Geothermics* 51:113–123. doi: 10.1016/j.geothermics.2013.10.012

## APPENDIX

### Appendix 1: Mineral phases of the basalt specific mineral set, grouped according to the structure.

mineral group	associated mineral phases
carbonates	calcite, aragonite
oxides and hydroxides	hematite, goethite
sulfides and sulfates	pyrite, marcasite, pyrrhotite, anhydrite, gypsum
sorosilicates	epidote
inosilicates	anthophyllite, tremolite, pargasite
phyllosilicates	illite, smectite, clinochlore
tectosilicates	quartz, chalcedony, albite, K-feldspar, microcline, analcime, laumontite, wairakite